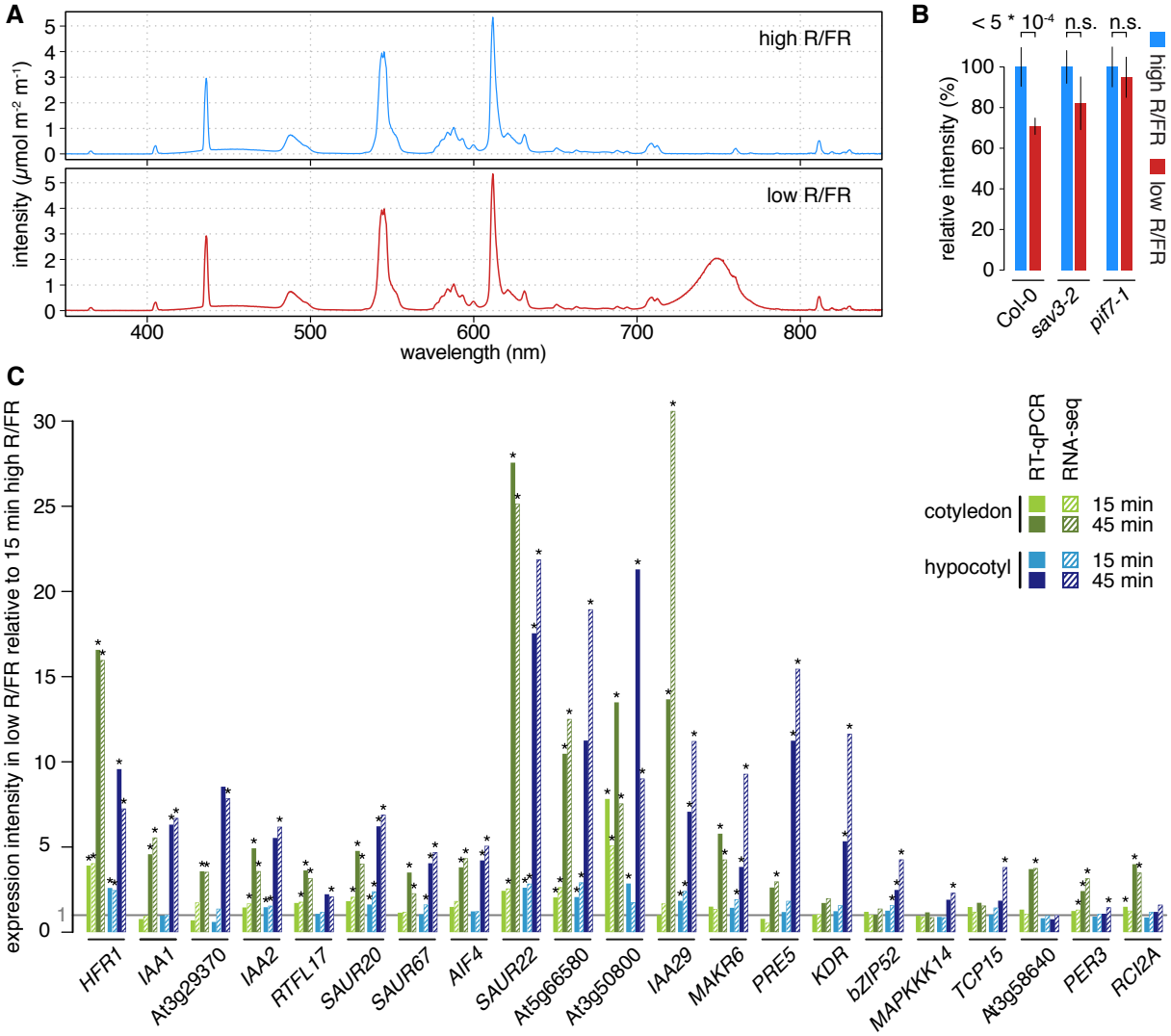

Supplemental Figure 1. Data validation and quantification.
(A) Light spectra (350–850 nm) of the high and low R/FR conditions used in this publication. (B) DII-VENUS signal intensity is significantly reduced by 1 h low R/FR in the wild type but not in *sav3-2* and *pif7-1*. The signal intensity was quantified in the upper part of hypocotyls and represented relative to a high R/FR control. Error bars indicate ± 2× SEM; Student's t-test: n.s. = not significant ($p > 0.05$); $n \geq 5$ (C) RNA-seq and RT-qPCR analyses show similar transcriptional responses. Data are represented as ratio between expression intensity in low R/FR relative to 15 min high R/FR. Significantly shade-regulated genes analyzed by RNA-seq are marked with an asterisk. RT-qPCR data were analyzed with Student's t-test (⋆: $p < 0.05$).

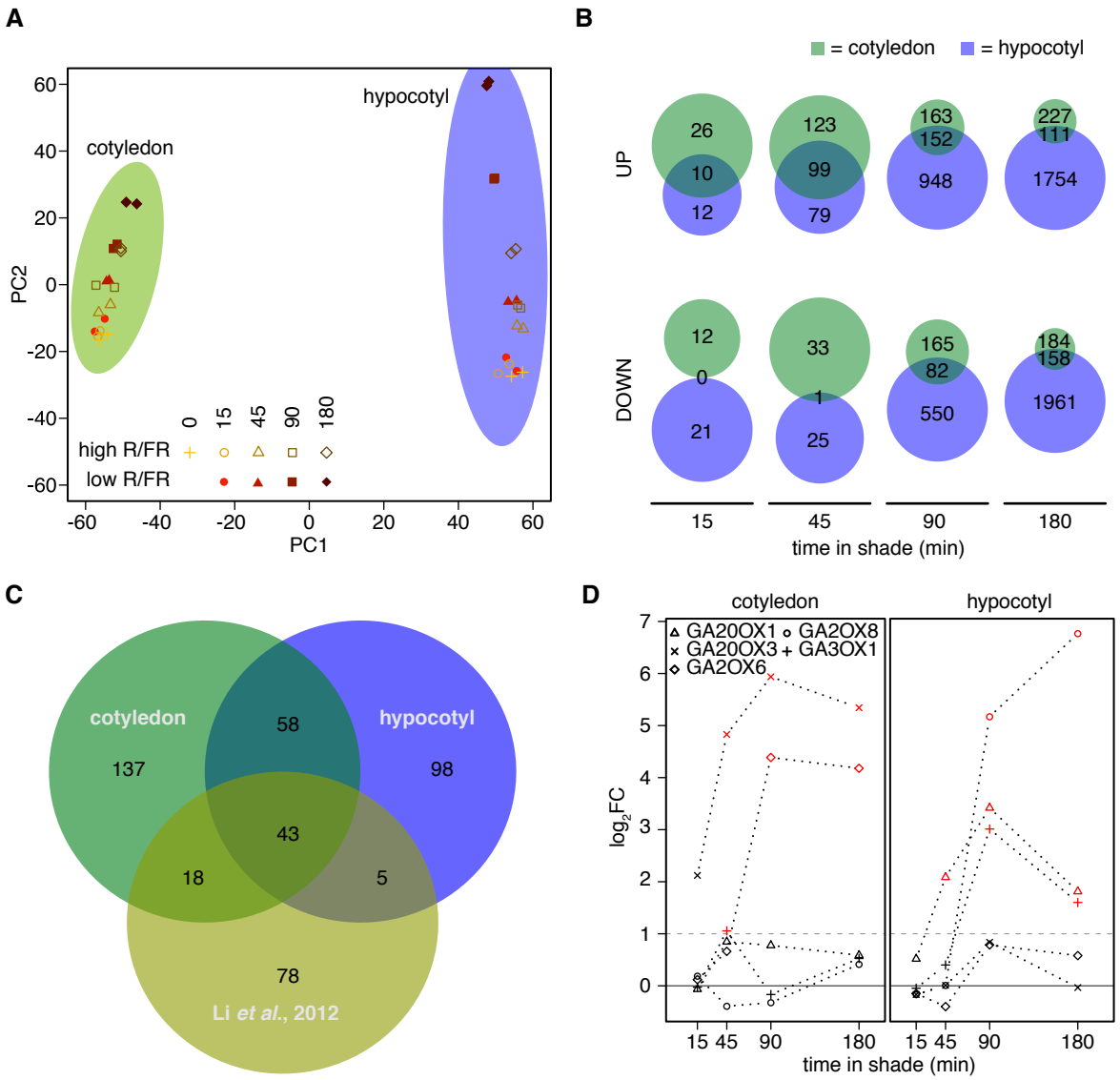

Supplemental Figure 2. Transcriptional regulation in shade shows organ-specific traits.
(A) Principal component analysis of RNA-seq libraries using the 5000 genes with the highest variation across libraries. Principal component (PC) 1 and PC2 are graphically visualized. (B) Venn diagrams of significantly shade-regulated genes in cotyledon and hypocotyl samples at different time points. (C) Set analysis between significantly regulated genes in cotyledon and hypocotyls after 45 min in shade and previously identified shade-regulated genes in whole seedlings by (Li et al., 2012). (D) RNA-seq analysis of transcriptional regulation of selected genes involved in later steps of the gibberellic acid biosynthetic pathway. Measurements with 2-fold change threshold with an adjusted p value < 0.01 are indicated with a red symbol.

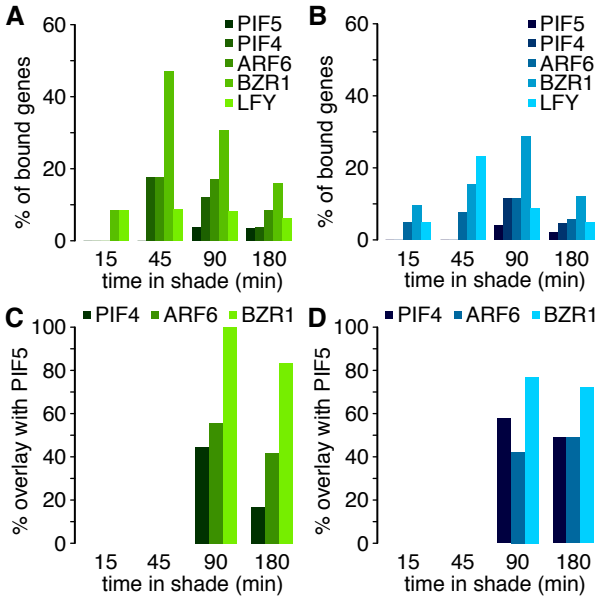

Supplemental Figure 3. Binding of PIF4, PIF5, ARF6, BZR1 and LFY to shade-repressed genes in hypocotyls and cotyledons.

Relative number of DTG among shade-repressed genes in the cotyledon (A) and hypocotyl (B). (C, D) Overlap between shade-repressed DTG of PIF4 and ARF6 relative to shade-repressed DTG of PIF5 in the cotyledon and hypocotyl, respectively.

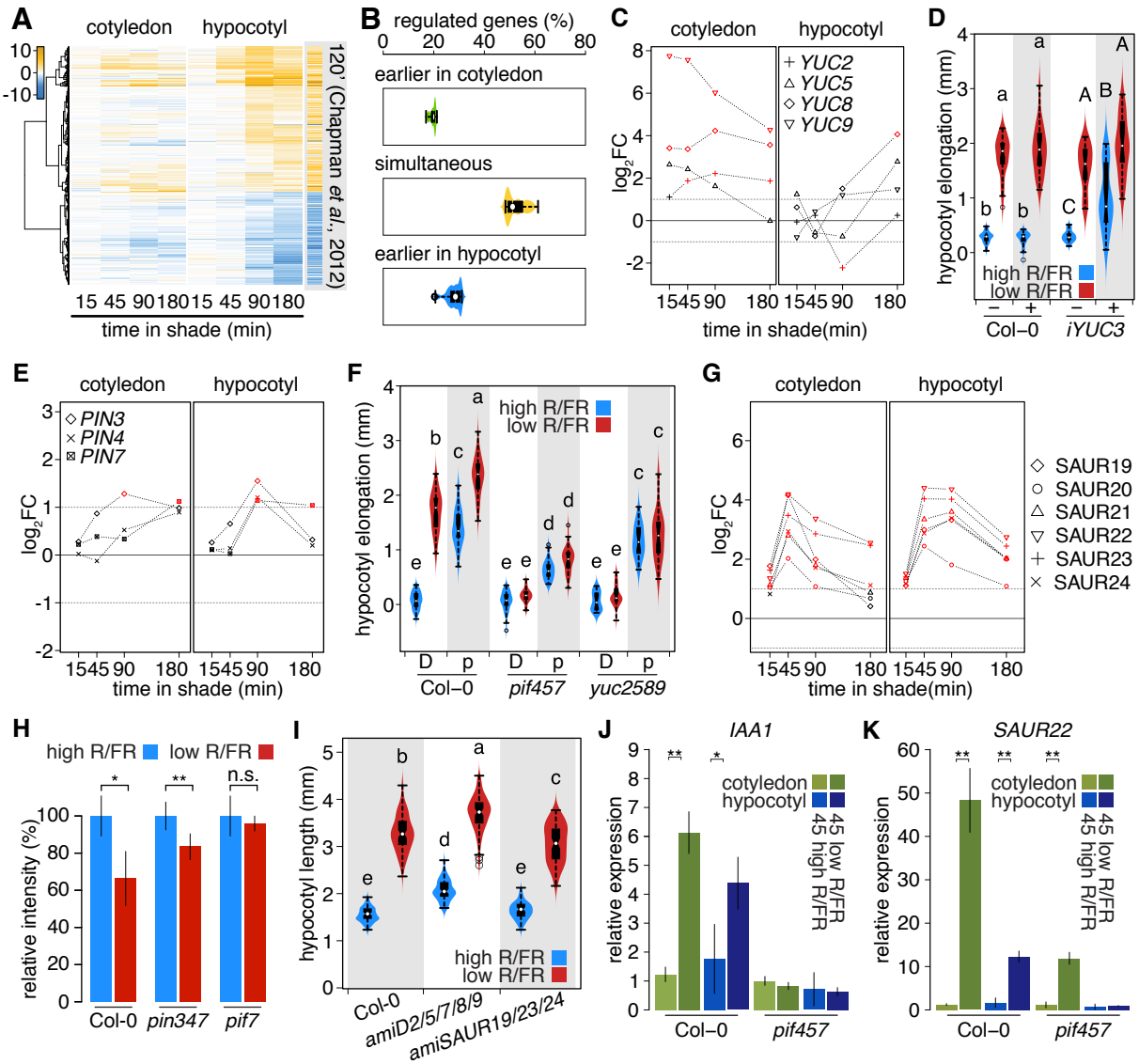

Supplemental Figure 4. Different types of shade-regulation among typical auxin response genes.
(A) Hierarchical clustering of shade-regulated genes reported as picloram-inducible in hypocotyls after 120 min. Each gene was significantly enriched in at least one condition. (B) Repeated classification of auxin-inducible genes in respect to their transcriptional response to shade using a range of 0.05 ≥ adj. p ≥ 0.001 as criteria. (C), (E) and (G) RNA-seq analysis of transcriptional ratio between high and low R/FR of selected *YUCCA*, *PIN* and *SAUR19* gene family members, respectively. Measurements with 2-fold change threshold with an adjusted p value < 0.01 are indicated with a red symbol. (D) Hypocotyl elongation of Col-0 or *iYUC3* during 3 days of estradiol (+) or mock (–) treatment in high or low R/FR (n > 25). (F) Hypocotyl elongation on DMSO or picloram (D or p, respectively) during 3 days in high or low R/FR (n > 20). (H) DII-VENUS signal intensity in hypocotyls expressed relative to the control condition of different genotypes (n ≥ 4). (I) Hypocotyl elongation after 4 days in high R/FR followed by 3 days in high or low R/FR in Col-0 and amiRNA expressing lines targeted against the PP2C phosphatase or *SAUR19* subfamily (n > 80). (J and K) RT-qPCR analysis of auxin-inducible genes in Col-0 and *pif457* performed with three biological replicates and three technical repeats. P value for significance of difference in mean (t-test) is given above the bars in H, J and K. * < 0.05; ** < 0.01; n.s. = not significant. Error bars in H, J and K indicate ± 2x SEM. In D, F and I, data are represented as box plots and distribution of measurements (violin plot). Different letters indicate significant differences (Anova; significance level = 0.01).

A

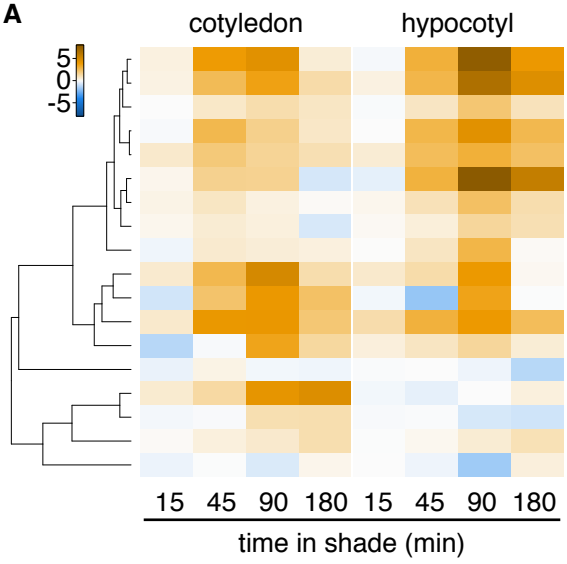

B

	time	cor
SAUR	early	0.757
	late	0.334
IAA	early	0.685
	late	0.351

C

	common	add. reg.
SAUR	26	25
IAA	2	16

Supplemental Figure 5. Shade regulation of the early auxin response in cotyledons versus hypocotyls.
(A) Hierarchical clustering of transcriptional ratios of IAA genes responding at least in one condition. (B) Pearson's correlation coefficient of transcriptional ratios of regulated *SAUR* or *IAA* genes between cotyledon and hypocotyl for 15 and 45 min (early) and 90 and 180 min (late). (C) Number of common and additional shade-responsive *SAUR* or *IAA* genes compared to 30 min picloram-regulated genes as reported by (Chapman et al., 2012).

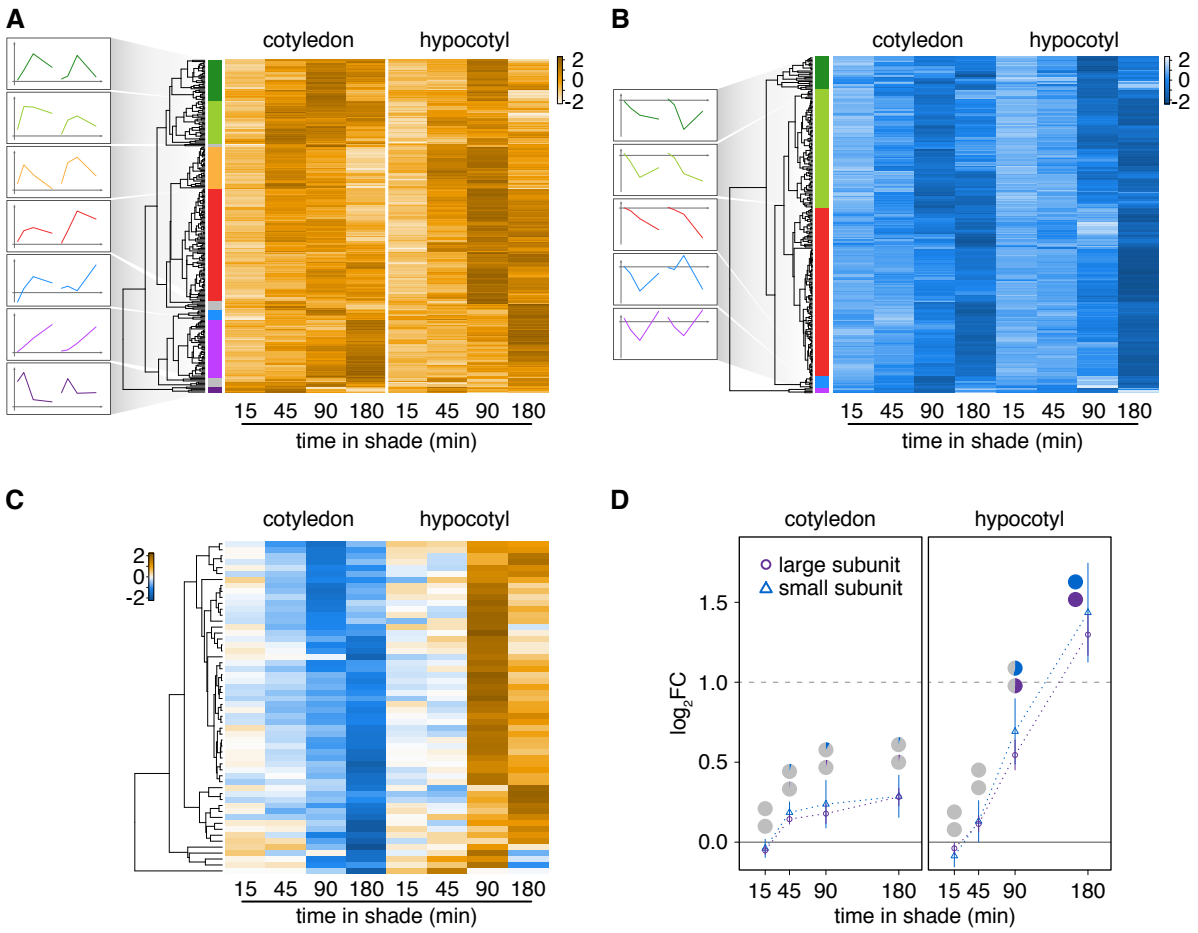

Supplemental Figure 6. Response patterns of genes regulated by shade in both hypocotyls and cotyledons.

Hierarchical clustering of shade-induced genes in both organs (A), shade-repressed genes in both organs (B) or genes being downregulated in cotyledon while upregulated in hypocotyl (C). (D) Average response patterns of 24 or 62 shade-regulated genes encoding for ribosomal proteins of the samll or large subunit, respectively. Pie charts represent the percentage of significantly regulated genes (2-fold change threshold with an adjusted p value < 0.01). Error bars = 2× SEM

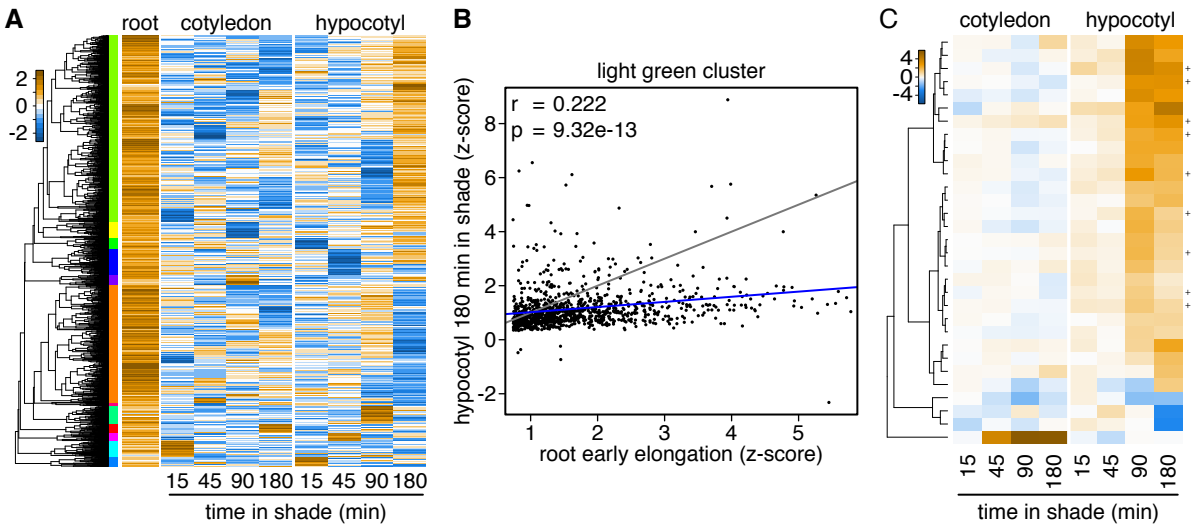

Supplemental Figure 7. A set of genes with similar expression patterns in the root elongation zone and shade-treated hypocotyls.

Hierarchical clustering of z-score normalized transcriptional ratios for upregulated genes in the early elongation zone vs. meristematic zone in roots and their corresponding regulation by shade (A). The z-score values of upregulated genes both in roots and hypocotyls after 180 min in shade (large light green cluster) and their correlation are shown in (B). Gray line: axes bisecting line; blue line: line of best fit (C) Hierarchically clustered logFC of shade-regulated members of the AGP family. PIF5 target genes are marked with a plus.

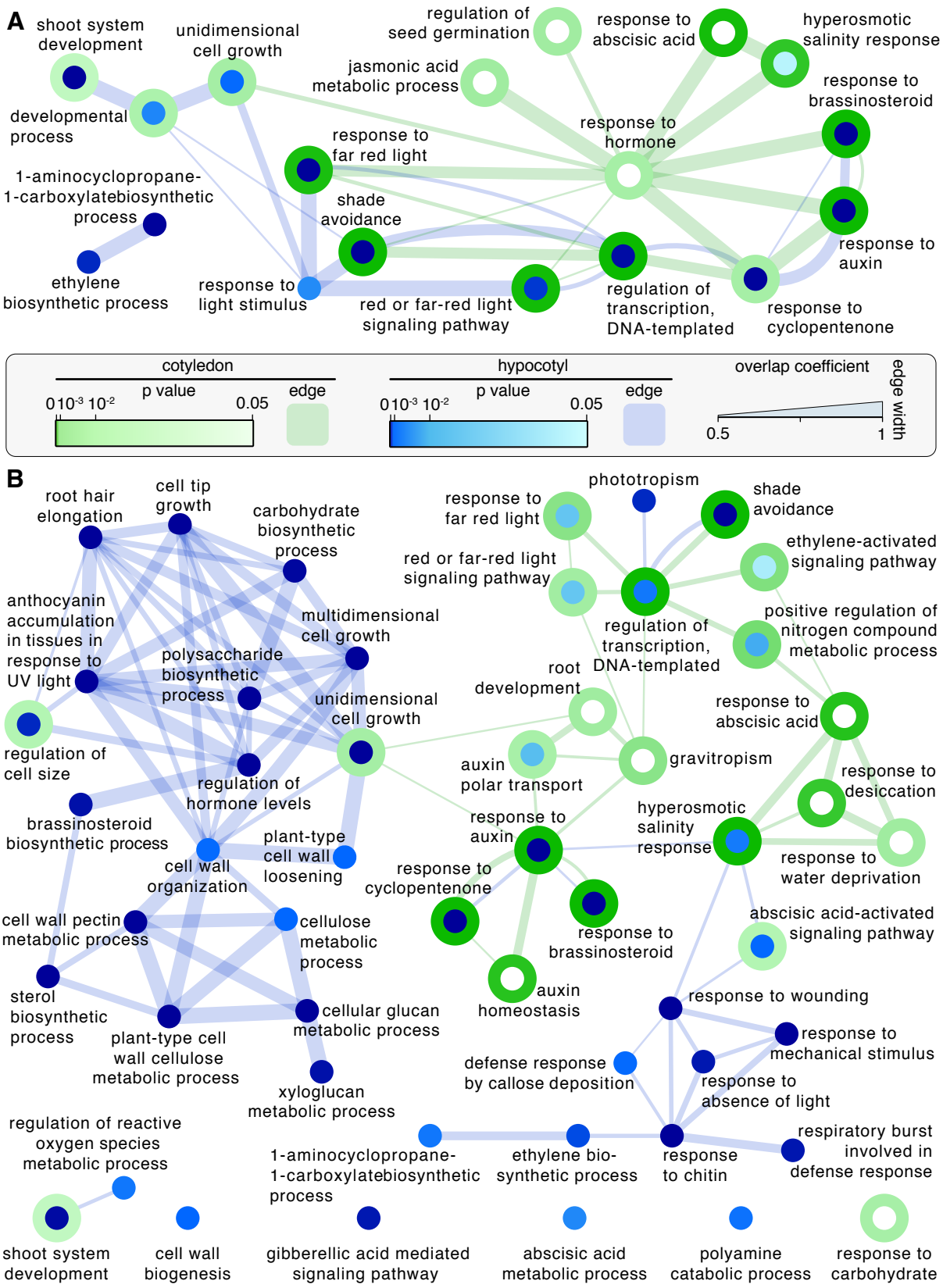

Supplemental Figure 8: Similarity networks of Gene Ontology terms become increasingly more organ specific with time in the shade.

Enrichment maps for upregulated genes after 45 min (A) and 90 min (B) in low R/FR. Nodes are colored in shades of green (outer ring) or blue (center) according to the GO terms significance of enrichment in cotyledon or hypocotyl, respectively. The overlap of significantly regulated genes is represented by the edge-weight in green or blue referring to identified GO terms in cotyledon or hypocotyl, respectively.

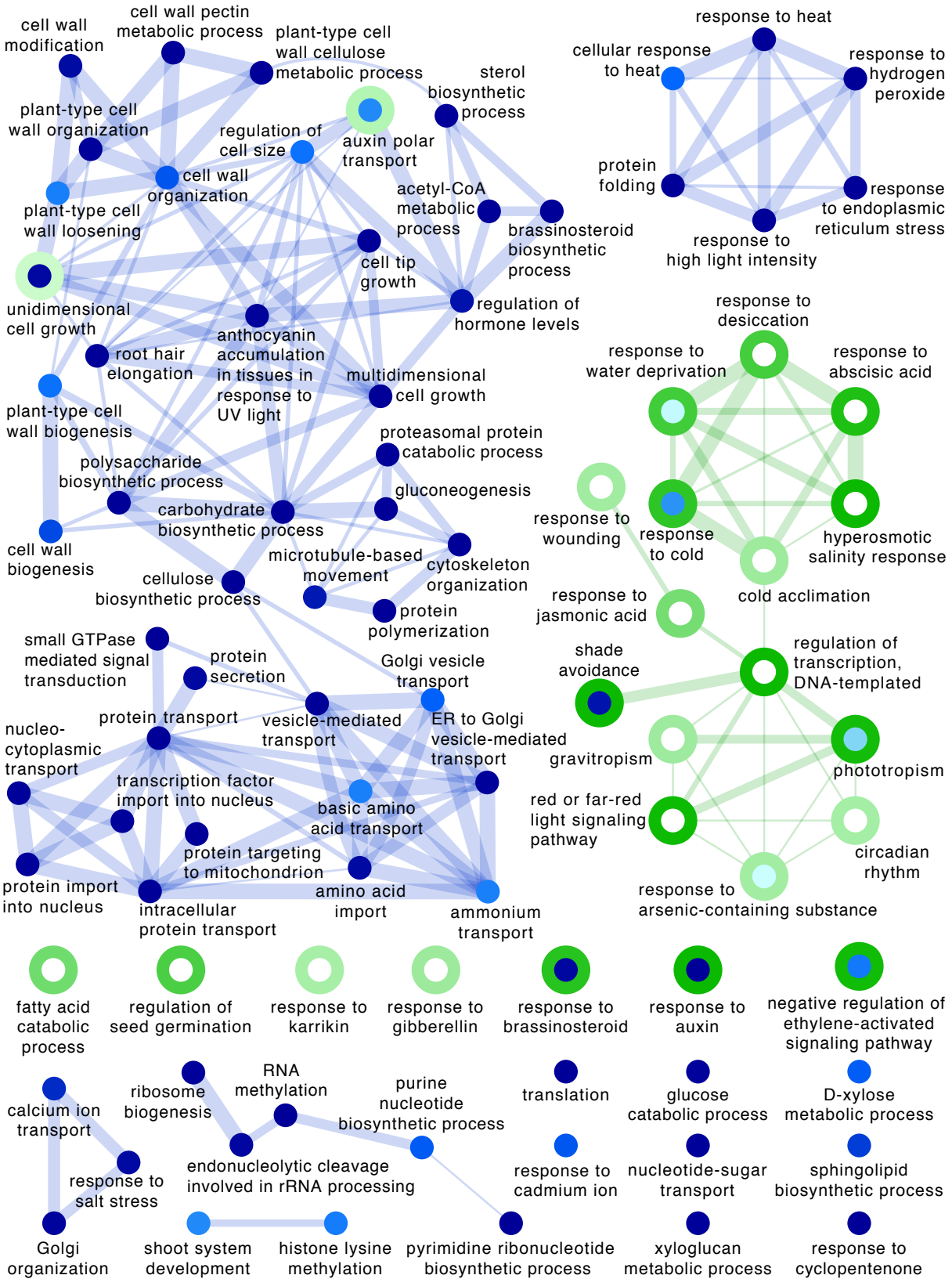

Supplemental Figure 9: Similarity networks of Gene Ontology terms.
Enrichment maps for upregulated genes after 180 min in low R/FR. The figure was designed similarly as Figure S8.

Supplemental Table 1: Primer sequences used for RT-qPCR

mRNA target symbol	AGI	Forward primer	Reverse primer
IAA1	At4g14560	GCTTCGTTTGGGATTACC	AGGAGGAGCAGATTCTTC
SAUR22	At5g18050	GTATGAGAGTGGCACTAAG	GCTCTGGTGAGAAGTCTAC
RTFL17	At1g13245	AATATTGCCCTCTCCTCCAC	TGTGGATGAATCGGTTAAGAG
SAUR67	At1g29510	CTCTTTCTTTCTCCACACTTTG	GGAGAGTTAAAGCTTGAGATTG
ACT2	At3g18780	GGTGATGGTGTGTCTCACACTGT	ATCAGTAAGGTCACGTCCAGCAA
PEX4/UBC21	At5g25760	CAGTCTGTGTGTAGAGCTATCATAGCAT	AGAAGATTCCCTGAGTCGCAGTT
YLS8	At5g08290	TCATTCGTTTCGGCCATGA	CTCAGCAACAGACGCAAGCA

Supplemental Methods

Plant growth, pharmacological treatments and growth analysis

Seeds were size selected and surface-sterilized using 70% (v/v) ethanol and 0.05% (v/v) Triton X-100 for 3 min followed by 10 min incubation in 100% (v/v) ethanol. Seeds were sowed on half-strength Murashige and Skoog medium (½ MS) containing 0.8% (w/v) phytoagar (Agar-Agar, plant; Roth) and subsequently stratified at 4 °C for 3 day in darkness. For experiments where seedlings were grown on vertical plates the phytoagar concentration was raised to 1.6% (w/v). Seedlings were grown in 16 h : 8 h, light : dark photoperiod (LD) at 21 °C in a Percival Scientific Model AR-22L (Perry, IA, USA) incubator. High R/FR was emitted from white fluorescence tubes (Lumilux cool white 18W/840) at a fluence rate of 130 μmol m^{-2} s^{-1} and low R/FR was achieved by supplementing high R/FR with 45 μM m^{-2} s^{-1}FR light (LEDs) lowering the R (640–700 nm):FR (700–760 nm) from 1.4 to 0.2, as measured by Ocean Optics USB2000+ spectrometer. Seedlings were grown for 4 days in high R/FR and subsequently kept in high R/FR or transferred to low R/FR for additional 3 days. Pharmacological treatments were done on vertically-grown seedlings on nylon meshes. After 4 days in white light (high R/FR) the seedling on nylon meshes were transferred to new plates containing the drug or the corresponding solvent and put for 3 additional days into high or low R/FR. Picloram was solved in DMSO (dimethylsulfoxide) and applied at a concentration of 10 μM. Estradiol was used at a concentration of 10 μM and solved in EtHO (ethanol). DP (α,α-dipyridyl) was dissolved in DMSO and applied at 5 μM, 10 μM or 25 μM. The effect of DP on hypocotyl elongation was measured after 1 day to minimize potential light degradation of DP (Velasquez et al., 2011). For end point measurements seedlings were imaged on a flatbed scanner (600 dpi) and the hypocotyl length was determined using ImageJ (http://rsb.info.nih.gov/ij) or a MATLAB script provided by Dr. Prashant Saxena. For time lapse imaging analysis seedlings were grown for 5 days on vertical plates. On day 6, seedlings were either maintained in high R/FR or transferred to low R/FR 2 h after the light onset (ZT2). Seedlings were imaged by time-lapse photography in intervals of 30 min using a Canon EOS 550D camera, equipped with a 50 mm macro-

objective and computer piloted using the DSLR Remote Pro Multi-Camera (v. 1.7.2) software (Breeze Systems). Hypocotyl length was measured by means of a semi-automated MATLAB script provided by Dr. Tino Dornbusch. Values for new growth were obtained by subtracting the hypocotyl length at ZT2.5. The length was smoothed with a sliding window approach averaging the length of three consecutive time points for visualization only.

Microscopy

Four days old seedlings grown as described above where either put for 1 hour into low R/FR light condition before confocal acquisition or kept in high R/FR. The microscope used is an inverted Zeiss confocal microscope (LSM 710 INVERTED, × 20 objective). VENUS signal was detected using an Argon laser (excitation at 514 nm and band pass emission between 520 and 560 nm). Image stacks were acquired for every hypocotyl. The pinhole was opened to collect the maximal signal intensity together with the minimal stack number (20.2 µm section, 12.08 µm interval). Images were processed with ImageJ software (http://rsb.info.nih.gov/ij). To quantify the VENUS signal, we used the SUM slices projection of 4 slices from the stack. We then selected a ROI in the upper part of the hypocotyl and got ride of all the stomata manually before measuring the signal intensity (raw integrated density).

RNA-seq analysis

Purity-filtered reads were adapters and quality trimmed with Cutadapt (v. 1.2.1) and the parameter -O 6 -q 20 and filtered for low complexity with PrinSeq (v. 0.20.3. (Schmieder and Edwards, 2011); parameters: -min_len 40 -lc_method dust -lc_threshold 7). Reads were aligned against the *Arabidopsis thaliana* (TAIR10) genome using Tophat (v. 2.0.9. (Kim et al., 2013)) and the parameters --bowtie1 --read-edit-dist 3 --read-realign-edit-dist 0 -library-type fr-firststrand. More than 25 million uniquely mapped reads were obtained per library that correspond to a more than 20 times genome coverage. The number of read counts per gene locus was summarized with htseq-count (v. 0.5.4p3, (Anders et al., 2015), parameters: -s reverse) using TAIR10 gene annotation. Quality of the RNA-seq data alignment was assessed using RSeQC (v. 2.3.7, (Wang et al., 2012)).

Statistical analysis was performed in R (v. 3.1.2, RCoreTeam2015). Genes with low counts (< 50 counts across all samples) were filtered out. Library sizes were scaled using TMM normalization (EdgeR v. 3.4.0; (Robinson et al., 2010)) and variance stabilized with limma's voom function (v. 3.18.2; (Law et al., 2014)). Differential expression was computed with limma (v. 3.18.2; (Ritchie et al., 2015)) by fitting data into a linear model. Limma uses empirical Bayesian methods to share information between genes; in particular, the estimated variability for a given gene borrows information from the other genes (Ritchie et al., 2015). As such, even if measurements are made in duplicate, the variability is calculated using data from all samples (18 conditions in duplicates). This method prevents many false positives, by ensuring that the variability for a given time point cannot be below the variability observed for other data points. This was demonstrated in a recent study by Schurch et al (2016) that showed that limma could control the false positive rate (FPR) at < 5% even with duplicates (Schurch et al., 2016). For each comparison a moderated t-test was used and adjusted p-values were computed by the Benjamini-Hochberg method, controlling for false discovery rate (FDR). RNA-seq data have been deposited in the National Center for Biotechnology Information's Gene Expression Omnibus as GEO series GSE81202.

ChIP-seq analysis

In order to improve our comparisons, all ChIP-seq datasets were reanalyzed using methods similar to a recently described bioinformatics pipeline (Heyndrickx et al., 2014) The following ChIP-seq datasets were reanalyzed: PIF5: (Hornitschek et al., 2012) (SRP010315); PIF4: (Oh et al., 2012) (SRX117693); ARF6: (Oh et al., 2014) (SRX368984); BZR1: (Oh et al., 2014) (upon request); LFY: (Moyroud et al., 2011) (SRR070383). The ChIP-seq data were analyzed according to the pipeline presented in (Heyndrickx et al., 2014) with slight modifications regarding the software versions. Reads were assessed for quality using FASTQC (v. 0.11.2;(Patel and Jain, 2012)), trimmed with fastx-toolkit (v. 0.0.13.2; http://hannonlab.cshl.edu/fastx_toolkit/; -Q33) and finally mapped onto the TAIR10 genome using BWA (v. 0.7.5a; (Li and Durbin, 2009)). The obtained

BAM files were sorted and cleaned using samtools (v. 0.1.19; (Li et al., 2009)). Duplicates were removed with Picard-Tools (v. 1.130; http://picard.sourceforge.net). Peak calling of mapped NGS reads was performed with MACS2 (v. 2.1.0; (Zhang et al., 2008) parameters: -g 1.0e8 and FDR < 0.05). The nearest genes were obtained using bedtools (v. 2.22.1;(Quinlan and Hall, 2010); closest -D "b") and the TAIR10 gene annotation.

Comparisons with published datasets

Raw data from root tissues (Wilson et al., 2015) were obtained through ArrayExpress (www.ebi.ac.uk; E-MEXP-2912). The wild-type samples from this dataset were pulled in form of .cel files and their quality evaluated using simpleaffy (v. 2.46.0; (Wilson and Miller, 2005)) and affy (v. 1.48.0;(Gautier et al., 2004)). The sample DZ_1 (1st replicate from late elongation samples) was found to show elevated features of RNA degradation and was removed prior further analysis. The samples were normalized using GCRMA and analyzed for differential gene expression analysis with the limma (v. 3.26.9; (Wettenhall and Smyth, 2004)) package in R. Differentially regulated genes for the early root elongation zone were obtained comparing meristematic tissue and early elongation tissue. Further analyses were limited to significantly differentially expressed genes with a cut-off of 2-fold differential expression and an adjusted p value threshold of 0.01.

List of hormone regulated genes were obtained from (Goda et al., 2008). The significance of the overlap with shade responsive genes were determined using a hypergeometric test with a significance threshold of 2.5×10^{-4}. The correlation quality was accessed using the cor.test function in R (v. 3.2.4).

Gene identifiers of ribosomal proteins were obtained from (Hummel et al., 2015). Genes of hormone biosynthetic pathways were obtained form the web site of the RIKEN institute on 17 March 2016 (http://hormones.psc.riken.jp/pathway_hormones.shtml).

In the context of this analysis ‘auxin responsive genes’ were defined as a pooled set of genes that respond to the synthetic auxin analog picloram (Chapman et al., 2012) or applied IAA (Nemhauser et al., 2006). Using low

significance thresholds (FC > 1.5; adj. p value < 0.05) 539 auxin responsive genes showed a response to low R/FR at least at time point per organ. Those genes were subsequently classified in three categories: 1) earlier response in cotyledon than hypocotyl, 2) earlier response in hypocotyl than cotyledon and 3) detection at similar time points. All observed combinations of time points per category were pooled and expressed relative to the number of classified genes in total. Finally, this classification was repeated testing 7029 combinations of significance criteria ($1.5 \leq FC \leq 5$, increments of 0.05; $0.05 \geq$ adj. p value ≥ 0.001, decrements of 5×10^{-4}) or a sole adj. p value cutoff (decrements of 5×10^{-5}).

Cluster analysis

All hierarchical clustering was done with the heatmap.2 (v. 2.17.0) function of the statistical environment R (v. 3.1.1,). LogFC-values were clustered using the ward.D2 algorithm and the Euclidean distance. Z-score values were clustered using average linkage and Pearson's correlation coefficient as distance metric. For the time course analysis data were partitioned into four groups prior to clustering. Genes which responded at least at one time point and organ to low R/FR classified into the following groups: not regulated, cotyledon specific regulated, hypocotyl specific regulated or regulated in both organs. Low R/FR responsive genes were further subdivided according to the direction of their regulation. To this end genes were clustered with the heatmap.2 function and split into two groups base on their logFC change. The fold changes were then transformed into z-score values and newly clustered. Clusters of response pattern were defined guided by the dendrogram and color coded in the row side bar. Few genes (gray) were not assigned to any cluster. The average response pattern were calculated per cluster and positioned in a schematic coordinated system based on an overlay of the similar response pattern calculated with an additional fixed fold change of 1 for 0 min in shade.

Gene set enrichment analysis for Gene Ontology

Gene set enrichment analysis were conducted with topGo (topology-based Gene Ontology scoring v. 2.20.0), (Alexa et al., 2006) using the gene

annotation provided by the org.At.tair.dp package (v. 3.1.2) and Gene Ontology (GO) definition of the GO.db package (v. 3.1.2). The analysis was performed using the Fisher statistic and the weight01 algorithm. GO terms with less than 4 annotated genes were excluded from the analysis.

Similarity networks of enriched GO categories were visualized with Enrichment Map (v. 2.1; GO-category p-value cut-off 0.005; overlap-coefficient cut-off 0.5; (Merico et al., 2010)) and Cytoscape (v. 3.4). Nodes are colored according to the enrichment p-value of the underlying GO-term in the TopGo analysis. The edge weight proportionally represents the overlap coefficient between GO terms.

References

Alexa, A., Rahnenfuhrer, J., and Lengauer, T. (2006). Improved scoring of functional groups from gene expression data by decorrelating GO graph structure. Bioinformatics **22,** 1600-1607.

Anders, S., Pyl, P.T., and Huber, W. (2015). HTSeq--a Python framework to work with high-throughput sequencing data. Bioinformatics **31,** 166-169.

Chapman, E.J., Greenham, K., Castillejo, C., Sartor, R., Bialy, A., Sun, T.P., and Estelle, M. (2012). Hypocotyl transcriptome reveals auxin regulation of growth-promoting genes through GA-dependent and -independent pathways. PloS one **7,** e36210.

Gautier, L., Cope, L., Bolstad, B.M., and Irizarry, R.A. (2004). affy--analysis of Affymetrix GeneChip data at the probe level. Bioinformatics **20,** 307-315.

Goda, H., Sasaki, E., Akiyama, K., Maruyama-Nakashita, A., Nakabayashi, K., Li, W., Ogawa, M., Yamauchi, Y., Preston, J., Aoki, K., Kiba, T., Takatsuto, S., Fujioka, S., Asami, T., Nakano, T., Kato, H., Mizuno, T., Sakakibara, H., Yamaguchi, S., Nambara, E., Kamiya, Y., Takahashi, H., Hirai, M.Y., Sakurai, T., Shinozaki, K., Saito, K., Yoshida, S., and Shimada, Y. (2008). The AtGenExpress hormone and chemical treatment data set: experimental design, data evaluation, model data analysis and data access. The Plant journal : for cell and molecular biology **55,** 526-542.

Heyndrickx, K.S., Van de Velde, J., Wang, C., Weigel, D., and Vandepoele, K. (2014). A functional and evolutionary perspective on transcription factor binding in Arabidopsis thaliana. The Plant cell **26,** 3894-3910.

Hornitschek, P., Kohnen, M.V., Lorrain, S., Rougemont, J., Ljung, K., Lopez-Vidriero, I., Franco-Zorrilla, J.M., Solano, R., Trevisan, M., Pradervand, S., Xenarios, I., and Fankhauser, C. (2012). Phytochrome interacting factors 4 and 5 control seedling growth in

changing light conditions by directly controlling auxin signaling. The Plant journal : for cell and molecular biology **71,** 699-711.

Hummel, M., Dobrenel, T., Cordewener, J.J., Davanture, M., Meyer, C., Smeekens, S.J., Bailey-Serres, J., America, T.A., and Hanson, J. (2015). Proteomic LC-MS analysis of Arabidopsis cytosolic ribosomes: Identification of ribosomal protein paralogs and re-annotation of the ribosomal protein genes. Journal of proteomics **128,** 436-449.

Kim, D., Pertea, G., Trapnell, C., Pimentel, H., Kelley, R., and Salzberg, S.L. (2013). TopHat2: accurate alignment of transcriptomes in the presence of insertions, deletions and gene fusions. Genome biology **14,** R36.

Law, C.W., Chen, Y., Shi, W., and Smyth, G.K. (2014). voom: Precision weights unlock linear model analysis tools for RNA-seq read counts. Genome biology **15,** R29.

Li, H., and Durbin, R. (2009). Fast and accurate short read alignment with Burrows-Wheeler transform. Bioinformatics **25,** 1754-1760.

Li, H., Handsaker, B., Wysoker, A., Fennell, T., Ruan, J., Homer, N., Marth, G., Abecasis, G., Durbin, R., and Genome Project Data Processing, S. (2009). The Sequence Alignment/Map format and SAMtools. Bioinformatics **25,** 2078-2079.

Merico, D., Isserlin, R., Stueker, O., Emili, A., and Bader, G.D. (2010). Enrichment map: a network-based method for gene-set enrichment visualization and interpretation. PloS one **5,** e13984.

Moyroud, E., Minguet, E.G., Ott, F., Yant, L., Pose, D., Monniaux, M., Blanchet, S., Bastien, O., Thevenon, E., Weigel, D., Schmid, M., and Parcy, F. (2011). Prediction of regulatory interactions from genome sequences using a biophysical model for the Arabidopsis LEAFY transcription factor. The Plant cell **23,** 1293-1306.

Nemhauser, J.L., Hong, F., and Chory, J. (2006). Different plant hormones regulate similar processes through largely nonoverlapping transcriptional responses. Cell **126,** 467-475.

Oh, E., Zhu, J.Y., and Wang, Z.Y. (2012). Interaction between BZR1 and PIF4 integrates brassinosteroid and environmental responses. Nature cell biology **14,** 802-809.

Oh, E., Zhu, J.Y., Bai, M.Y., Arenhart, R.A., Sun, Y., and Wang, Z.Y. (2014). Cell elongation is regulated through a central circuit of interacting transcription factors in the Arabidopsis hypocotyl. eLife **3**.

Patel, R.K., and Jain, M. (2012). NGS QC Toolkit: a toolkit for quality control of next generation sequencing data. PloS one **7,** e30619.

Quinlan, A.R., and Hall, I.M. (2010). BEDTools: a flexible suite of utilities for comparing genomic features. Bioinformatics **26,** 841-842.

Ritchie, M.E., Phipson, B., Wu, D., Hu, Y., Law, C.W., Shi, W., and Smyth, G.K. (2015). limma powers differential expression analyses for RNA-sequencing and microarray studies. Nucleic acids research **43,** e47.

Robinson, M.D., McCarthy, D.J., and Smyth, G.K. (2010). edgeR: a Bioconductor package for differential expression analysis of digital gene expression data. Bioinformatics **26,** 139-140.

Schmieder, R., and Edwards, R. (2011). Quality control and preprocessing of metagenomic datasets. Bioinformatics **27,** 863-864.

Schurch, N.J., Schofield, P., Gierlinski, M., Cole, C., Sherstnev, A., Singh, V., Wrobel, N., Gharbi, K., Simpson, G.G., Owen-Hughes, T., Blaxter, M., and Barton, G.J. (2016). How many biological replicates are needed in an RNA-seq experiment and which differential expression tool should you use? Rna **22,** 839-851.

Velasquez, S.M., Ricardi, M.M., Dorosz, J.G., Fernandez, P.V., Nadra, A.D., Pol-Fachin, L., Egelund, J., Gille, S., Harholt, J., Ciancia, M., Verli, H., Pauly, M., Bacic, A., Olsen, C.E., Ulvskov, P., Petersen, B.L., Somerville, C., Iusem, N.D., and Estevez, J.M. (2011). O-glycosylated cell wall proteins are essential in root hair growth. Science **332,** 1401-1403.

Wang, L., Wang, S., and Li, W. (2012). RSeQC: quality control of RNA-seq experiments. Bioinformatics **28,** 2184-2185.

Wettenhall, J.M., and Smyth, G.K. (2004). limmaGUI: a graphical user interface for linear modeling of microarray data. Bioinformatics **20,** 3705-3706.

Wilson, C.L., and Miller, C.J. (2005). Simpleaffy: a BioConductor package for Affymetrix Quality Control and data analysis. Bioinformatics **21,** 3683-3685.

Wilson, M.H., Holman, T.J., Sorensen, I., Cancho-Sanchez, E., Wells, D.M., Swarup, R., Knox, J.P., Willats, W.G., Ubeda-Tomas, S., Holdsworth, M., Bennett, M.J., Vissenberg, K., and Hodgman, T.C. (2015). Multi-omics analysis identifies genes mediating the extension of cell walls in the Arabidopsis thaliana root elongation zone. Frontiers in cell and developmental biology **3,** 10.

Zhang, Y., Liu, T., Meyer, C.A., Eeckhoute, J., Johnson, D.S., Bernstein, B.E., Nusbaum, C., Myers, R.M., Brown, M., Li, W., and Liu, X.S. (2008). Model-based analysis of ChIP-Seq (MACS). Genome biology **9,** R137.